Effect of Nanoparticles on Gas Sorption and Transport in Poly(1-trimethylsilyl-1-propyne)

Timothy C. Merkel,* Zhenjie He, and Ingo Pinnau

Membrane Technology and Research, 1360 Willow Road, Menlo Park, California 94025-1516

Benny D. Freeman

Department of Chemical Engineering, Center for Energy and Environmental Resources, University of Texas at Austin, 10100 Burnet Road, Austin, Texas 78758

Pavla Meakin and Anita J. Hill

Division of Manufacturing and Infrastructure Technology, CSIRO, Private Bag 33, Clayton, VIC 3168 Australia

Received February 6, 2003; Revised Manuscript Received June 16, 2003

ABSTRACT: Penetrant permeability coefficients in high-free-volume, glassy poly(1-trimethylsilyl-1-propyne) [PTMSP] increase systematically with increasing concentration of nonporous, nanoscale fumed silica [FS]. For example, the permeability of PTMSP containing 40 wt % FS to methane is 180% higher than that of the unfilled polymer. Gas and vapor solubility in the nanocomposites are unaffected by FS at concentrations of up to 50 wt %. Penetrant diffusion coefficients in PTMSP increase with increasing FS content, and the enhanced permeability in the nanocomposites is due to this rise in diffusivity. These results are qualitatively similar to behavior previously observed when FS was added to another stiff-chain polyacetylene, poly(4-methyl-2-pentyne) [PMP]. However, in contrast to PMP, the permeability of PTMSP to relatively small gases increases more upon filling than that of larger penetrants. This results in a reduction in vapor/permanent-gas selectivity for filled PTMSP. In fact, mixed-gas *n*-butane/methane selectivity is 64% lower in PTMSP containing 50 wt % FS than in pure PTMSP. These results, combined with penetrant diffusion coefficients on the order of 10^{-3} cm^2/s in filled PTMSP, suggest an escalating influence of free phase transport mechanisms such as Knudsen diffusion as FS concentration in the polymer increases.

Introduction

Organic−inorganic hybrid membranes have received much attention in the past decade as potential "next generation" membrane materials for gas separations.[1−5] Such hybrid membranes are typically composed of porous inorganic zeolite particles dispersed in a polymeric matrix. In principle, these so-called "mixed matrix membranes" can combine the excellent size-sieving capacity of zeolites with the desirable mechanical and processing attributes of polymers. However, attaining this synergy is difficult. Frequently, mixed matrix membranes fail to exhibit their theoretical separation performance due to the formation of relatively nonselective defects at the interface between the zeolite particles and the polymer medium. Such difficulties have hindered commercial development and implementation of mixed matrix membranes.[4,5]

Recently,[6−9] the addition of nonporous, nanometer-scale fumed silica [FS] particles to high-free-volume, glassy poly(4-methyl-2-pentyne) [PMP] was discovered to simultaneously increase both permeability and vapor/permanent-gas selectivity. For example, incorporation of 30 wt % FS into PMP doubles mixed-gas *n*-butane/methane selectivity and increases *n*-butane permeability by a factor of 3. These results are particularly unusual because the addition of nonporous fillers typically reduces polymer permeability and has little effect on selectivity.[10,11] Positron annihilation lifetime spectroscopy [PALS] results suggest that the FS particles enhance free volume in the polymer phase of the nanocomposite, which increases diffusion coefficients and decreases polymer size selectivity.[7,9] Consequently, when PMP is filled, the permeability of relatively large vapor molecules (e.g., *n*-C_4H_{10}) is enhanced more than that of smaller permanent gases (e.g., CH_4), leading to a significant increase in the vapor selectivity of PMP. In contrast to the role of zeolites in mixed matrix membranes, FS particles are nonporous and do not permeate gas molecules. Rather, when dispersed in rigid polymers the small size of FS primary particles (∼10−30 nm) apparently allows them to alter polymer chain packing and, thereby, permeation properties, without introducing gross defects or compromising a film's mechanical strength at loadings of up to 40−50 wt %.

PMP is a member of a family of substituted acetylene polymers that exhibit high permeability, and in many cases, they are vapor selective (i.e., they are more permeable to large organic vapors than to small permanent gases).[12] Vapor selectivity in glassy polymers is unusual (most conventional glasses are more permeable to small molecules than to larger ones), and this behavior in certain substituted polyacetylenes is attributed, in part, to the very high free volume in these polymers.[12] This high free volume results from inefficient polymer chain packing caused by a rigid, twisted polymer backbone, bulky pendant groups, and low interchain cohesion.[12] The high permeability and vapor selectivity of some polyacetylenes make them of interest in applications such as the selective removal of higher hydrocarbons from methane (i.e., natural gas dewpointing), organic monomer recovery from mixtures with nitrogen, and hydrocarbon removal from mixtures with

10.1021/ma0341566 CCC: $25.00
Published on Web 08/05/2003

hydrogen.[13] The most studied member of the polyacetylene family is poly(1-trimethylsilyl-1-propyne) [PTMSP], a material possessing the highest organic-vapor permeability and vapor/permanent-gas selectivity of all known polymers.[12,14−17] PTMSP is approximately an order of magnitude more permeable than PMP and has roughly double the vapor/permanent-gas selectivity of PMP. However, the industrial utility of PTMSP is limited, among other reasons, by its high solubility in hydrocarbon solvents, which can restrict its use in the hydrocarbon vapor environments where its transport properties would be most beneficial. For this reason, PMP, which has better solvent resistance than PTMSP, was selected as the matrix material for our first study of filled, high-free-volume, vapor-selective polymers. In light of the results obtained with PMP and given the structural similarity of the two polymers, it is of interest to understand whether the addition of FS to PTMSP produces transport effects similar to those reported in PMP. In this way, one may gain some insight into the nature and generality of the unusual transport behavior in filled, high-free-volume glassy polymers.

This study reports permeability, solubility, and diffusion coefficients of several gases and vapors in PTMSP and FS-filled PTMSP. The pressure and temperature dependence of permeability coefficients are reported as a function of FS content, yielding information regarding the effect of FS on transport mechanisms in PTMSP. These data are compared and contrasted with previous results for FS-filled PMP and interpreted in terms of the filler impact on polymer chain packing. To aid in this analysis, positron annihilation lifetime spectroscopy is utilized to examine the effect of FS concentration on polymer free volume.

Background

Transport in Dense Polymers. The permeability, P, of a polymer film to a penetrant is the pressure and thickness normalized flux:[18]

$$P = \frac{Nl}{p_2 - p_1} \tag{1}$$

where p_2 is the feed or upstream pressure, p_1 is the permeate or downstream pressure, l is the film thickness, and N is the steady-state penetrant flux through the polymer film. Permeability is frequently expressed in barrers, where 1 barrer $= 10^{-10}$ cm^3 (STP) cm/(cm^2 s cmHg).

Gas transport in nonporous polymers, as well as some microporous materials, proceeds by a solution-diffusion mechanism, for which the permeability coefficient may be expressed as[18]

$$P = \left(\frac{C_2 - C_1}{p_2 - p_1}\right)D \tag{2}$$

where D is the concentration-averaged effective diffusion coefficient and C_2 and C_1 are the penetrant concentrations in the polymer at the upstream (p_2) and downstream (p_1) faces of the membrane, respectively. When the downstream pressure is much less than the upstream pressure, eq 2 may be expressed as[18]

$$P = SD \tag{3}$$

where S is the solubility coefficient at the upstream pressure.

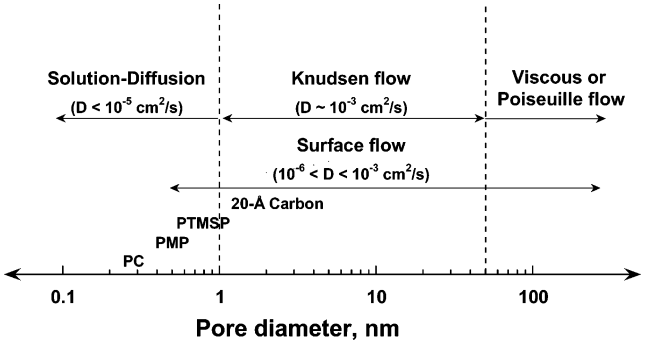

Figure 1. Transport regimes in polymers and 20 Å nanoporous carbon as a function of pore or free volume element diameter. The positions for PTMSP, PMP, and polycarbonate [PC] are estimated from literature PALS data.[7,50] The positions of the transport boundaries are discussed in refs 22−25 and roughly correspond to what would be expected at ambient temperature and pressure for a 3 Å diameter penetrant.

The ideal selectivity of a polymer film for component A relative to component B, $\alpha_{A/B}$, is the ratio of their permeabilities, which may be rewritten as the product of two terms:[18]

$$\alpha_{A/B} = \frac{P_A}{P_B} = \left(\frac{S_A}{S_B}\right)\left(\frac{D_A}{D_B}\right) \tag{4}$$

where the first term on the right-hand side is the solubility selectivity and the second is the mobility or diffusivity selectivity.

The temperature dependence of permeability, diffusivity, and solubility at temperatures removed from polymer thermal transitions is described as follows:[18]

$$P = P_0 \exp\left(-\frac{E_P}{RT}\right) \tag{5}$$

$$D = D_0 \exp\left(-\frac{E_D}{RT}\right) \tag{6}$$

$$S = S_0 \exp\left(-\frac{\Delta H_S}{RT}\right) \tag{7}$$

where P_0, D_0, and S_0 are preexponential constants, E_P is the activation energy of permeation, E_D is the activation energy of diffusion, ΔH_S is the enthalpy of sorption, R is the universal gas constant, and T is the absolute temperature. Because permeability is the product of solubility and diffusivity, the following relationship exists between the activation energies of permeation and diffusion and the enthalpy of sorption:

$$E_P = E_D + \Delta H_S \tag{8}$$

Transport in Microporous Materials. Previous studies of PTMSP suggest that this polymer contains relatively large, interconnected free volume elements (diameter ~ 1 nm) rendering PTMSP films microporous.[12] As such, PTMSP has been envisioned as a transitional material, where molecular transport may occur by pore flow mechanisms as well as by the solution-hindered diffusion mechanism prevalent in conventional dense polymers.[19−21] This point is demonstrated in Figure 1, which illustrates the different types of transport that may occur through a material as a function of the pore or free volume element size in the material. The boundaries between transport regimes are, in reality,

not as sharply defined as shown in Figure 1 and, of course, depend on conditions such as temperature and pressure as well as the interconnectivity of free volume elements and penetrant molecule size.[22−25] Nevertheless, the figure is useful to show that whereas traditional dense polymers such as polycarbonate fall exclusively in the solution diffusion realm, PTMSP, by virtue of its large free volume elements, inhabits a region where additional transport mechanisms may be operative.

Penetrant molecules can potentially encounter several different regions in PTMSP: (1) the dense polymer matrix, within which transport would occur by the conventional solution diffusion route; (2) pore walls, along which penetrant can sorb and be transported by surface diffusion[26] (this mechanism would be most significant for condensable, highly sorbing vapors); and (3) continuous channels, through which nonsorbed penetrant may be transported by a pore flow mechanism such as Knudsen diffusion (or Poiseuille flow if the pores are very large). In pore flow, if the mean free path of a molecule is long relative to the pore diameter, collisions with the pore wall will be more common than those with other gas molecules, and Knudsen flow will predominate.[27] Knudsen diffusion separates penetrants on the basis of differences in molecular weight, and consequently, small permanent gases are always transported more rapidly by this mechanism than larger vapor molecules.[28] In comparison, solution-diffusion transport can be vapor selective, as is observed for some weakly size-sieving, high-free-volume polymers (e.g., PTMSP). Additionally, solution-diffusion diffusivities in polymers are typically less than 10^{-5} cm^2/s (compared with values on the order of 10^{-3} cm^2/s for Knudsen diffusion) and in contrast to Knudsen flow, solution-diffusion transport is an activated process.[18,28]

Transport in Heterogeneous Materials. Many theoretical expressions[11] have been developed to describe transport behavior in heterogeneous polymer systems. A frequently used example of such a model is that due to Maxwell, which was originally proposed for analyzing the specific electrical resistance of a compound medium consisting of a dilute suspension of spheres.[29] Applied to permeation in a binary system consisting of a nonporous, nonsorbing, impermeable filler dispersed in a continuous polymer matrix, the permeability of the composite is

$$P = P_p\left(\frac{1-\phi_f}{1+\frac{\phi_f}{2}}\right) \tag{9}$$

where P_p is the permeability of the pure polymer and ϕ_f is the volume fraction of filler. Mathematically, eq 9 indicates that the permeability of the filled polymer is always less than that of the pure polymer and decreases with increasing filler concentration. This trend is typically observed in conventional filled polymers,[11,30] where the primary effect of the filler particles is to increase the tortuosity for diffusion and decrease the effective solubility of the composite, thereby reducing permeability. Of course, the model would not be valid if the presence of filler particles disturbs the permeation properties of the polymer or if the particles aggregate and/or polymer chains desorb from the particle surface, leading to voids around the particles. This appears to be the case for FS-filled PMP where filler addition induces an increase in permeability, contrary to the Maxwell prediction.[9]

Gas solubility in a binary system consisting of filler particles and polymer is typically described using the following additive model:[31]

$$S = \phi_p S_p + (1-\phi_p)S_f \tag{10}$$

where S_p is solubility in the polymer matrix, S_f refers to the gas solubility in the pores (for porous fillers) and on the surface of filler particles, and ϕ_p is the volume fraction of polymer. Frequently, if a filler is nonporous and interacts favorably with the polymer matrix such that it is fully wetted by polymer chains, sorption by the filler is very small, and the second term on the right-hand side of eq 10 is negligible.[31] Alternatively, additional complexity may be encountered if filler particles cluster together such that voids or gaps form between them where no polymer can access or, for example, if the filler induces morphological changes in the polymer matrix.[11]

Free Volume. Molecular diffusion through a dense polymer depends strongly on the amount of free volume that a material possesses.[18] Free volume, existing as static voids created by inefficient chain packing or transient gaps generated by thermally induced chain rearrangement, provides diffusing molecules with a low-resistance path for transport. The larger and more numerous free volume elements are, the faster molecules migrate through a polymer. Free volume also affects gas solubility in a polymer, although to a much weaker extent than its influence on diffusion.[32] Typically, solubility increases slightly with increasing polymer free volume. As a result, permeability, a composite property composed of contributions from solubility and diffusivity, increases with polymer free volume in a manner similar to that of diffusivity.[32]

The most common means of estimating polymer free volume is to calculate the fractional free volume via density measurements and group contribution methods. Previously, it was shown that it is difficult to detect changes in free volume caused by FS addition to PMP by this technique.[9] Instead, positron annihilation lifetime spectroscopy was used successfully to probe free volume changes in FS-filled PMP.[9] PALS provides an estimate of the size and concentration of both static and dynamic free volume elements in condensed matter (pure or heterogeneous).[33] In this method, a positron is injected into a sample, forms a spin parallel bound state with an electron called orthopositronium [oPs], and subsequently annihilates with an antiparallel electron of the surrounding medium to form γ-rays. The lifetime of an oPs particle depends on the electron density of its local environment, which is sensitive to the size of the free volume element in which it resides. The intensity of oPs annihilations is related to the concentration of accessible free volume elements. Numerous studies, including the recent examination of FS-filled PMP,[9] point to a strong correlation between PALS accessible free volume and polymer transport properties.[32,34,35]

Experimental Section

Film Preparation. Dense polymer/filler nanocomposite films were prepared by solution-casting mixtures of fumed silica and poly(1-trimethylsilyl-1-propyne) in a manner analogous to that used to prepare PMP/silica nanocomposites.[7,9] Synthesis and characterization information for PTMSP are provided elsewhere.[12] The polymer was dissolved in toluene

to give a 1.7 wt % polymer solution, which is near the solubility limit for PTMSP in this solvent and yields a viscous solution. The high solution viscosity helps inhibit gravity-driven settling of FS particles during film drying. Nonporous, hydrophobic FS powder (Cab-O-Sil TS-530, a grade of FS available from Cabot Corp., Tuscola, IL) was added to the polymer solution. TS-530 FS has a specific gravity of 2.2 g/cm^3 and a BET surface area of 230 m^2/g.[36] This surface area corresponds to an equivalent spherical primary particle diameter of 13 nm.[9] TS-530 FS has been chemically treated with hexamethyldisilazane to replace hydrophilic hydroxyl surface groups with hydrophobic trimethylsilyl surface groups.[36] Polymer, solvent, and FS were mixed at 18 000 rpm for 10 min in a Waring two-speed commercial blender. The blended mixture was filtered, poured into a casting ring, covered to permit slow solvent evaporation, and dried at ambient conditions until all solvent was removed. For PTMSP and the nanocomposites, this drying period was approximately 1 week. The films used in the permeation and sorption experiments were about 100 μm thick as determined by a precision micrometer. All experiments were conducted immediately following film drying to mitigate the effects of physical aging.[37] To ensure that aging effects did not obscure the results, nitrogen permeability and sorption measurements were conducted on samples before and after testing of other gases and were found to be consistent within experimental uncertainty.

Throughout this work the concentration of FS in PTMSP nanocomposite films is reported in weight percent. However, for comparison with literature data pertaining to transport in filled polymers where fillers of different densities have been used, it is more appropriate to express filler content on a volumetric basis. Accordingly, the FS volume fraction in PTMSP has been estimated using pure component densities as follows:

$$\phi_f = \frac{w_f}{w_f + \frac{\rho_f}{\rho_p}(1 - w_f)} \tag{11}$$

Here, ρ_p and ρ_f denote the pure polymer and filler densities, respectively, and w_f is the filler weight fraction.

Permeation Measurements. The pure gas permeation properties of PTMSP and FS-filled nanocomposites were determined with a constant pressure/variable volume apparatus.[38] The surface area of the film was 13.8 cm^2, and gas flow rates were measured with a soap-film bubble flowmeter. Prior to each experiment, both the upstream and downstream sides of the permeation cell were purged with penetrant gas. Permeability coefficients of gases and vapors were determined in the order of increasing penetrant condensability, i.e., H_2, N_2, CH_4, C_2H_6, C_3H_8, n-C_4H_{10}. When steady-state conditions were achieved, the following expression was used to evaluate permeability:[38]

$$P = \frac{l}{p_2 - p_1}\frac{273}{TA}\frac{p_{atm}}{76}\left(\frac{dV}{dt}\right) \tag{12}$$

where p_2 is the upstream pressure, p_1 is the downstream pressure (atmospheric pressure in this case), p_{atm} is atmospheric pressure (cmHg), A is the membrane area, T is absolute temperature (K), and dV/dt is the volumetric displacement rate of the soap film in the bubble flowmeter.

Mixed-gas permeation properties of films were determined with a feed containing 2 vol % n-butane in methane. The feed pressure in these experiments was 11.2 atm, and the permeate pressure was atmospheric. The ratio of permeate to feed flow rate, or stage cut, was always less than 1%. Under these conditions the residue and feed compositions are essentially equal. The permeate composition was determined with a gas chromatograph equipped with a thermal conductivity detector. Mixed-gas permeability coefficients for n-butane and methane were determined from the following relationship:

$$P = \frac{x_{perm} l}{x_{feed} p_2 - x_{perm} p_1}\frac{273}{TA}\frac{p_{atm}}{76}\left(\frac{dV}{dt}\right) \tag{13}$$

where x_{feed} and x_{perm} refer to the mole fractions of the penetrant of interest in the feed and permeate streams, respectively.

Sorption Measurements. The solubility of gases in PTMSP and the FS-filled nanocomposites was measured with a high-pressure barometric sorption apparatus.[39] Initially, the film to be studied was placed in a sample chamber and exposed to vacuum overnight to remove air gases. Penetrant gas was introduced into the chamber and allowed to equilibrate. Once the chamber pressure was constant, additional penetrant was introduced and equilibrium was reestablished. In this incremental manner, penetrant uptake was measured as a function of penetrant pressure. Sorption equilibrium for all gases was reached within, at most, a few hours. The experimental temperature was maintained to within ±0.1 °C with a constant temperature water bath.

Positron Annihilation Lifetime Spectroscopy. The PALS measurements were performed in N_2 at ambient temperature using an automated EG&G Ortec fast-fast coincidence system. The timing resolution of the system was 240 ps determined using the prompt curve from a ^{60}CO source with the energy windows set to ^{22}Na events. Polymer films approximately 50 μm thick were stacked to a total thickness of 1 mm on either side of the 30 μCi ^{22}Na−Ti foil source. From 5 to 15 spectra were collected for each sample with a 1 h acquisition time required per spectrum. These results were averaged to yield mean values. The standard deviations were the population standard deviations for nine spectra, and each spectrum consisted of approximately 1 million integrated counts. The PALS parameters for the spectra did not vary as a function of contact with the radioactive source. The spectra were modeled as the sum of four decaying exponential terms using the computer program PFPOSFIT. While the PALS signatures of most polymers can be modeled using three decaying exponential terms, a four-parameter fit gave better statistical results for the materials discussed in this work. The shortest lifetime was fixed at 125 ps, which is characteristic of parapositronium self-annihilation. No source correction was used in the analysis based on a fit for pure Al standards of 169 ± 2 ps, 99.3 ± 0.3%; 820 ps, 0.7%. Only the orthopositronium (oPs) components with the longest measured lifetimes—the third (τ_3) and fourth (τ_4)—were considered further since they are ascribed to annihilations in free volume cavities of the polymer matrix.

Results and Discussion

Positron Annihilation Lifetime Spectroscopy. Figure 2 presents oPs lifetimes in PTMSP as a function of FS content. As discussed previously, the longer the average lifetime of oPs probe particles in a sample, the larger the average size of free volume elements in the polymer. For most polymers, PALS spectra are described by a single oPs lifetime, τ_3. However, extremely high-free-volume polymers possess a second, longer oPs lifetime, τ_4.[34] It has been suggested that τ_4 corresponds to large, possibly interconnected free volume elements in substituted acetylene polymers such as PTMSP.[35] The current PALS analysis of PTMSP and FS-filled PTMSP indicates that these materials possess a bimodal distribution of oPs lifetimes. On the basis of the data in Figure 2, the shorter oPs lifetimes (τ_3) appear to be nearly independent of FS concentration, whereas the longer lifetimes (τ_4) increase with increasing FS content. This result indicates that large free volume elements in PTMSP increase in size with increasing FS concentration. Similar PALS results were previously observed in FS-filled PMP, where it was shown that the subtle

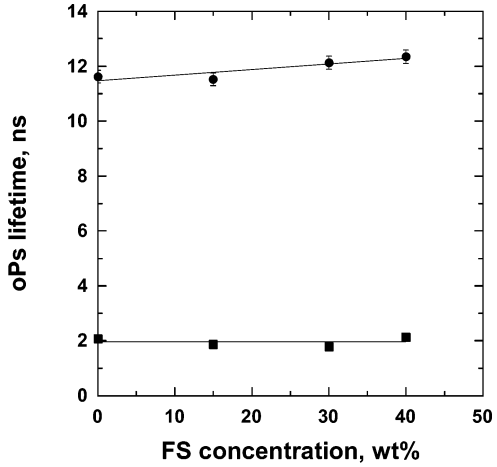

Figure 2. Effect of FS content on oPs lifetimes in PTMSP. PALS spectra were collected at ambient temperature in a nitrogen environment and modeled as the sum of four decaying exponential terms using the computer program PFPOSFIT.

increase in free volume detected by PALS resulted in significant increases in penetrant permeability and diffusion coefficients.

Permeability. Figure 3 presents pure-gas H_2, CH_4, C_2H_6, C_3H_8, and *n*-C_4H_{10} permeability coefficients in PTMSP containing varying amounts of FS as a function of penetrant transmembrane pressure difference, Δp. The permeability of unfilled PTMSP to each of these penetrants is very high, consistent with previous reports for this polymer[15,40] and the fact that PTMSP is the most permeable polymer known.[26,41] On the basis of the data in Figure 3, the addition of FS to PTMSP produces an even more permeable material. This result is in contrast to behavior in traditional filled polymer systems where filler addition reduces permeability.[10] The systematic increase in permeability exhibited by filled PTMSP is qualitatively similar to results obtained previously when FS was incorporated into another substituted polyacetylene, PMP.[9] For PMP, the increase in permeability upon filling was attributed to increased free volume in the FS-filled nanocomposites as compared to the unfilled polymer.[9] Presumably, by inhibiting efficient packing of rigid PMP chains, FS particles generate more spacious pathways for molecular transport. The PALS and permeation data illustrated in Figures 2 and 3 suggest that FS addition has a similar effect on the microstructure of PTMSP.

The penetrant permeability coefficients in Figure 3 exhibit a variety of pressure dependencies. For the light gases, hydrogen and methane, permeability coefficients do not depend appreciably on pressure in either PTMSP or the PTMSP/FS nanocomposites. This behavior is typical for these penetrants in PTMSP[40] and, in general, for low-sorbing, permanent gases in rubbery and glassy polymers.[42] Ethane permeability coefficients decrease monotonically with increasing upstream pressure in both PTMSP and FS-filled PTMSP. This behavior is frequently observed for more soluble, nonplasticizing penetrants in glassy polymers and is usually ascribed to the saturation of sorption sites associated with the nonequilibrium excess volume of the glassy polymer and resultant decrease in solubility with increasing penetrant pressure.[43]

For larger, strongly sorbing propane and *n*-butane, the pressure dependence of permeability varies with FS content. Propane permeability coefficients increase with increasing Δp in PTMSP containing 0 and 30 wt % FS, which is typical for a plasticizing penetrant in a glassy polymer.[44] However, in PTMSP containing 40 wt % FS, propane permeability initially decreases and then increases slightly with increasing Δp at transmembrane pressures greater than approximately 4 atm. Finally, in a sample containing 50 wt % FS, propane permeability decreases monotonically with increasing Δp. That is, PTMSP becomes less susceptible to propane-induced plasticization as FS content increases. For *n*-butane permeability coefficients in PTMSP and the FS nanocomposites, permeability increases with increasing Δp, again suggesting penetrant-induced plasticization. As FS content in PTMSP increases, the increase in *n*-butane permeability with increasing Δp becomes smaller. For example, PTMSP permeability to *n*-butane increases from 48 000 to 83 000 barrers (a 73% increase) as Δp increases from 0.4 to 1.1 atm. Over the same pressure range, the permeability of PTMSP containing 50 wt % FS increases from 123 000 to 142 000 barrers (an increase of only 15%). Thus, for *n*-butane (just as for propane), FS addition to PTMSP decreases the extent to which permeability increases with increasing Δp. This result may be explained in terms of FS augmenting the size of free volume elements in PTMSP. Increased permeability at higher penetrant pressures is frequently attributed to penetrant-induced plasticization or swelling of the polymer matrix combined with increased local-scale segmental dynamics which facilitate penetrant diffusive jumps (and, in turn, increases permeability coefficients).[43] As polymer free volume increases, the capacity of the matrix to accommodate a given amount of penetrant without disruption of polymer chain packing should increase. Consequently, all other factors being equal (e.g., polymer cohesive energy density, etc.), plasticization of a glassy polymer and the associated increase in penetrant permeability at high Δp could be mitigated as polymer free volume increases, which is exactly what we observe in Figure 3.

Figure 4 presents methane permeability enhancement (i.e., the ratio of permeability in the filled polymer to that in the unfilled polymer) in PTMSP as a function of FS content. Also included in this figure are predictions from the Maxwell model, data for filled PMP,[9] and data for another filled polyacetylene, poly(1-phenyl-2-(*p*-(triisopropylsilyl)phenyl)acetylene) [PTPSDPA]. Like PMP and PTMSP, PTPSDPA is an amorphous, high glass transition temperature (T_g > 250 °C), vapor-selective glassy polymer.[45] The chemical structure of PTPSDPA is[45]

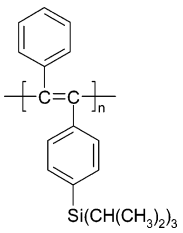

In contrast to PMP and PTMSP, PTPSDPA has a lower free volume and, consequently, is significantly less permeable than the other polymers.[45] In fact, the permeability of PTPSDPA to permanent gases is approximately an order of magnitude lower than that of PMP and 2 orders of magnitude less than PTMSP. As demonstrated in Figure 4, permeability behavior in filled PTMSP and PTPSDPA is similar to that in PMP

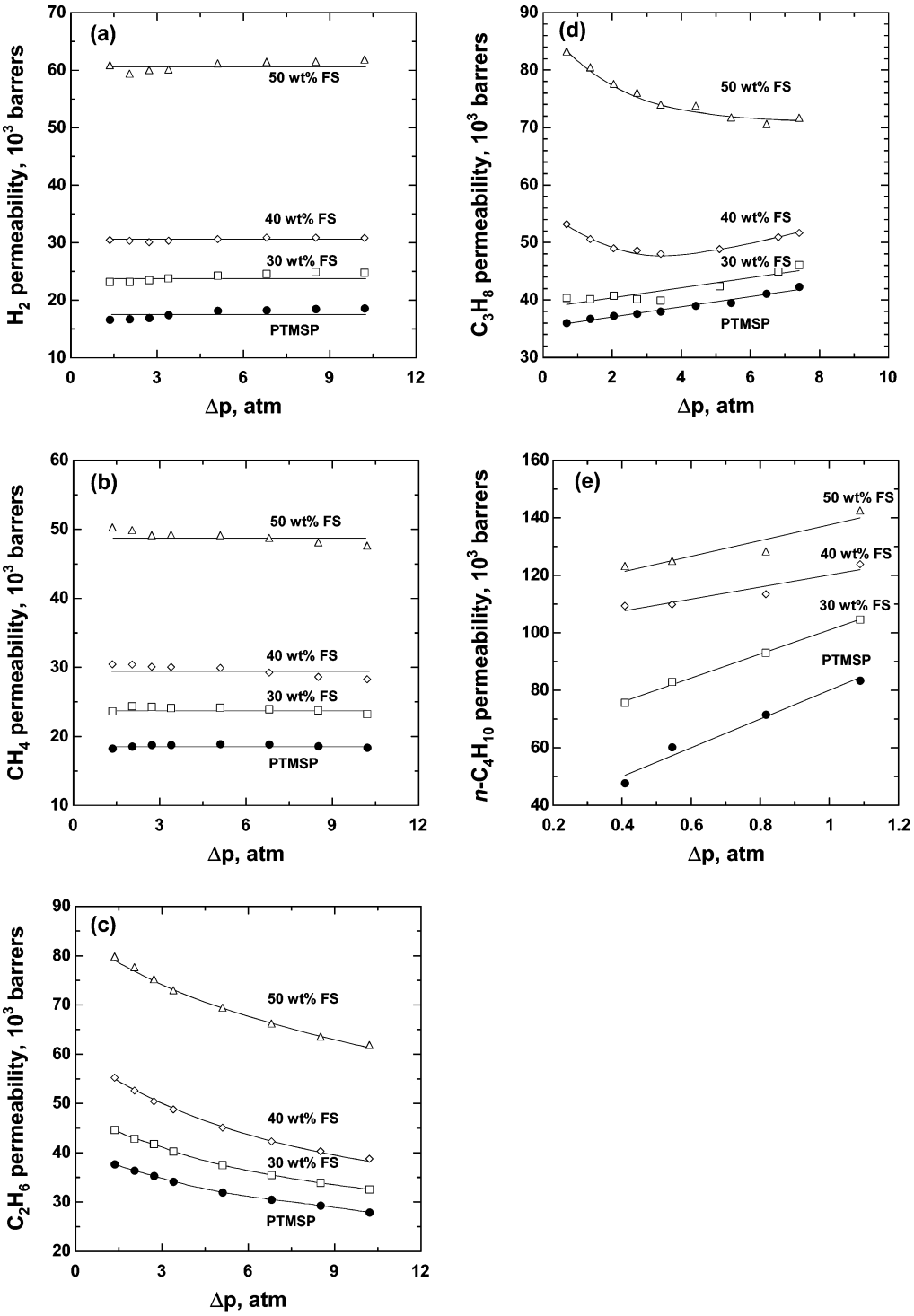

Figure 3. Permeability coefficients of (a) hydrogen, (b) methane, (c) ethane, (d) propane, and (e) *n*-butane in PTMSP containing 0, 30, 40, and 50 wt % FS at 25 °C.

and contrary to expectations for traditional filled systems. As in PMP, the dominant effect of FS addition to PTMSP and PTPSDPA is to increase penetrant transport. Any increase in the tortuosity of the diffusion path caused by the presence of impermeable FS particles appears to be more than offset by the apparent free volume increase caused by FS addition. On the basis of the data in Figure 4, at equivalent volume fractions of FS, permeability enhancement in the polyacetylenes is in the following order:

PTPSDPA > PMP > PTMSP

This result is opposite to the order of the base polymer permeability, indicating that at least for the materials considered in this study the increase in penetrant flux obtained by adding a given amount of FS decreases as the permeability of the polymer being filled increases. A correlation between unfilled polymer permeability and permeability enhancement upon filling is demonstrated in Figure 5. This behavior is probably related to the relative free volume of the polymers being filled and their ability to accommodate FS particles within the polymer matrix. On the basis of transport parameters and other estimates of free volume, such as PALS,

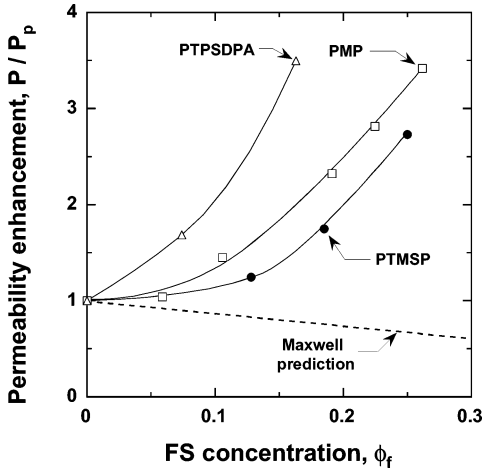

Figure 4. Ratio of methane permeability in the filled polymer to that in the unfilled polymer (i.e., permeability enhancement) as a function filler content. The dashed line represents the prediction of the Maxwell model (eq 9). For our PMP (□),[9] PTMSP (●), and PTPSDPA (△) data the filler was TS-530 FS, the measurement temperature was 25 °C, and the transmembrane pressure difference was 3.4 atm.

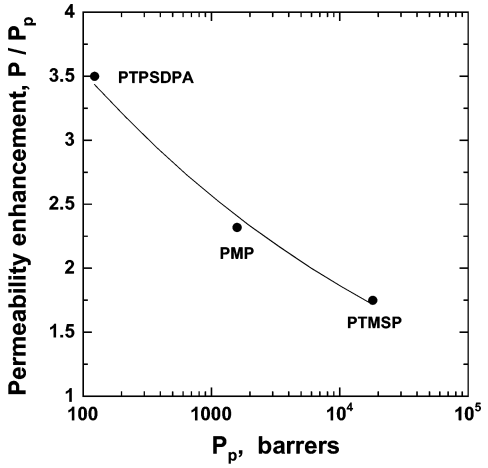

Figure 5. Ratio of permeability in the filled polymer to that in the unfilled polymer (i.e., permeability enhancement) as a function of the unfilled polymer permeability. These data are for methane permeation at 25 °C and a Δp of 3.4 atm.

PTMSP possesses the largest free volume elements among these polymers.[32,46] Consequently, PTMSP accommodates FS particles with the least disruption of polymer chain packing and experiences, therefore, the smallest permeability enhancement. Conversely, PTPSDPA has the lowest permeability and free volume among these polymers. It experiences the greatest chain packing disruption at a given volume fraction of FS, and it shows the largest permeability enhancement. Whether a correlation of the type demonstrated in Figure 5 can be extended to even lower free volume, conventional glassy polymers is unknown at this time.

Similar to results previously reported for PMP,[9] FS addition to PTMSP increases the permeability coefficients of different penetrants to different degrees. This finding is illustrated in Figure 6, which presents permeability enhancement in filled PTMSP as a function of penetrant size, characterized by critical volume, V_C. However, the effect of penetrant size on permeability enhancement is markedly different in the two polymers. For PMP, incorporation of FS into the matrix enhances the permeability of larger penetrants (e.g., *n*-C_4H_{10})

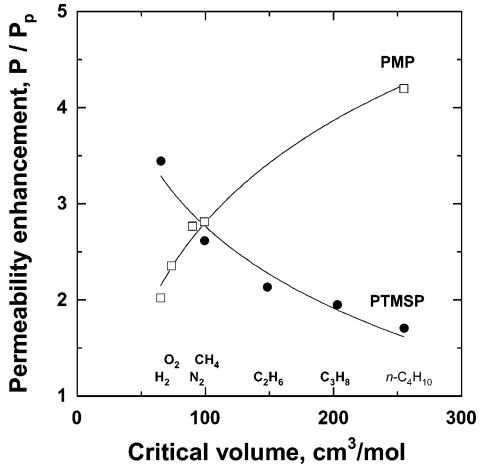

Figure 6. Permeability enhancement at 25 °C in PTMSP and PMP[9] as a function of penetrant size. PTMSP data (●) are from pure gas measurements at 4.4 atm upstream pressure (except *n*-butane, for which upstream pressure = 2.1 atm) in PTMSP containing 50 wt % FS and pure PTMSP. PMP data (□) are from pure gas measurements at 4.4 atm upstream pressure (except *n*-butane, which is from mixed gas data where the feed is 98 vol % methane and 2 vol % *n*-butane at a feed pressure of 11.2 atm and a permeate pressure of 1 atm) in PMP containing 45 wt % FS and pure PMP.

more than that of smaller gases (e.g., H_2), consistent with a decrease in polymer size selectivity as free volume is increased. In contrast, when PTMSP is filled with FS, the permeability enhancement decreases with increasing penetrant size, so the flux of smaller penetrants increases more with FS addition than that of larger penetrants. As a variety of data will show, this result appears to be related to PTMSP's extremely microporous nature, which, when augmented by FS addition, leads to an increasing influence of pore-flow transport mechanisms (e.g., Knudsen flow). As mentioned previously, PTMSP is envisioned as a transition material exhibiting behavior intermediate between dense polymers and microporous materials such as small pore carbons.[19,26] As FS addition increases accessible free volume in PTMSP, pore-flow transport mechanisms, including Knudsen diffusion, may become progressively more important. Under this scenario, as the size of effective pore radii increase, smaller molecules would gain access to these additional, relatively fast transport mechanisms first and experience a greater increase in flux with FS addition than larger penetrants (which might still be predominantly restricted to transport through relatively more densified regions of the polymer matrix).

In support of the hypothesis outlined in the previous paragraph, Figure 7 presents pure-gas H_2/CH_4 selectivity in PTMSP and PMP as a function of FS content. Both penetrants are supercritical gases at the experimental conditions. Therefore, any contribution from condensed-phase selective surface flow to penetrant transport should be minimal. This fact permits a more direct assessment of the relative influence of Knudsen and solution-diffusion transport in filled PTMSP and PMP. On the basis of the data in Figure 7, the transport behavior in the two polyacetylenes is quite different; H_2/CH_4 selectivity decreases with increasing FS content in PMP and increases with FS loading in PTMSP. From transport measurements, PMP is hydrogen selective ($P_{H_2}/P_{CH_4} = 2.1$) because while methane is more soluble than H_2 in PMP ($S_{H_2}/S_{CH_4} = 0.16$), H_2 is smaller than

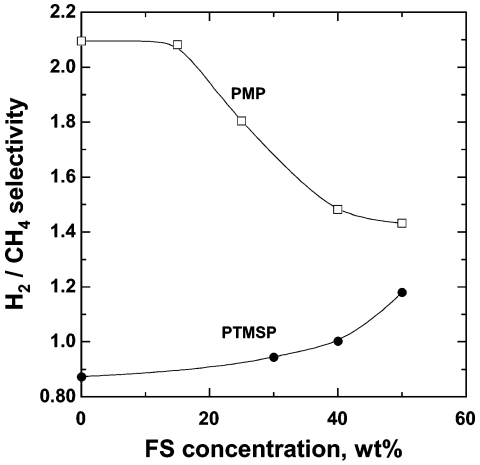

Figure 7. Pure-gas hydrogen/methane selectivity of PTMSP and PMP as a function of FS content. Measurements conducted at 25 °C and $\Delta p = 3.4$ atm.

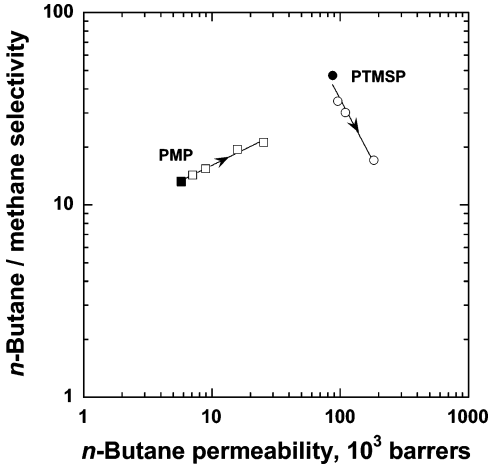

Figure 8. Mixed-gas *n*-butane/methane selectivity vs *n*-butane permeability in PTMSP (●), FS filled PTMSP (○; 30, 40, and 50 wt %), PMP (■), and FS filled PMP (□; 15, 25, 40, and 45 wt %). These data were acquired at 25 °C using a feed mixture containing 98 mol % methane in *n*-butane with an upstream pressure of 11.2 atm and a permeate pressure of 1 atm.

CH_4 and, consequently, has a significantly higher diffusion coefficient ($D_{H_2}/D_{CH_4} = 13$).[9] As FS content in PMP increases, H_2/CH_4 selectivity decreases by more than 30%. Since gas solubility in polymer/FS nanocomposites is relatively insensitive to FS concentration,[9] diffusivity selectivity must decrease as FS content increases, consistent with the notion that FS increases the free volume in PMP, thereby decreasing its size-sieving ability. Similar to PMP, CH_4 is more soluble than H_2 in PTMSP ($S_{H_2}/S_{CH_4} = 0.13$). However, PTMSP is more permeable to methane than to hydrogen ($P_{H_2}/P_{CH_4} = 0.88$) because the ratio of diffusion coefficients in PTMSP ($D_{H_2}/D_{CH_4} = 6.9$) is roughly half that in PMP. This difference in transport behavior for the base polymers is ascribed in part to the higher level of free volume in PTMSP and, consequently, its lower diffusivity selectivity than PMP.[14] As FS is added to PTMSP, H_2/CH_4 selectivity increases in the direction of the Knudsen selectivity for this gas pair (2.8). This result is consistent with the idea that FS addition to PTMSP diminishes the influence of solution diffusion transport, where the fact that methane is more soluble than hydrogen is important, and increases the influence of Knudsen transport, where solubility selectivity no longer plays a role (i.e., $S_{H_2}/S_{CH_4} = 1$ in a porous material where transport is via Knudsen diffusion). Consequently, PTMSP is methane selective without FS and becomes hydrogen selective after FS addition, and the H_2/CH_4 selectivity increases in the direction of the Knudsen limit.

Figure 8 presents mixed-gas *n*-butane/methane selectivity of PTMSP containing 0, 30, 40, and 50 wt % FS as a function of mixed-gas *n*-butane permeability. Data obtained under the same experimental conditions for PMP are included for comparison. As FS content increases, PTMSP's permeability increases while *n*-butane/methane selectivity decreases. The latter result is qualitatively different from the behavior of filled PMP, where both vapor selectivity and permeability are enhanced upon addition of FS to the polymer. This finding regarding the selectivity of PTMSP is consistent with the pure gas results that permeability of small molecules is augmented more than that of large molecules upon filling PTMSP with FS. Relative to pure PTMSP, *n*-butane/methane mixed-gas selectivity is 64% lower in PTMSP containing 50 wt % FS.

The reduction in vapor/permanent-gas selectivity for filled PTMSP suggests that FS creates free volume elements large enough to permit permanent-gas-selective Knudsen transport to be important. Further support for this hypothesis is provided from methane blocking data. Methane mixed-gas permeability coefficients in PTMSP are much lower than pure gas values when the copermeant in the mixed-gas feed is a condensable vapor, such as *n*-butane.[17] This transport behavior is similar to that exhibited by microporous carbon, where transport of condensable components occurs by surface diffusion along the walls of interconnected pores that span the membrane sample.[22] In mixed-gas feeds, the more condensable vapor will selectively sorb into these pores and by multilayer adsorption or capillary condensation effectively block the permeation of the less condensable gas through the pore structure.[22] In our experiments, the ratio of methane mixed-gas to methane pure-gas permeability (i.e., the blocking ratio) for unfilled PTMSP is 0.11, indicating that the presence of more condensable *n*-butane blocks nearly 90% of methane permeation. When FS is added to PTMSP, the methane blocking ratio changes. For example, at 50 wt % FS, this ratio increases to 0.21, indicating that *n*-butane is no longer able to block as much methane permeation as in pure PTMSP. This result may imply that the critical diameter of interconnected free volume elements in the 50 wt % FS film is increased such that in some of them sorbed *n*-butane is no longer able to span the free volume element and block methane permeation. This reduction in methane blocking and *n*-butane/methane selectivity for filled PTMSP suggests that the free volume of this material has exceeded a limit beyond which mechanisms adverse to the selective transport of large, condensable species are favored.

Figure 9 presents activation energies of permeation for several pure gases in PTMSP containing 0, 30, and 40 wt % FS. For each sample, E_P values decrease with increasing penetrant critical temperature, typical behavior for vapor-selective polymers where $|\Delta H_S| > E_D$.[14] FS addition to PMP systematically decreases E_P values, presumably due to increased polymer free volume, which reduces activation energies of diffusion.[9] In sharp

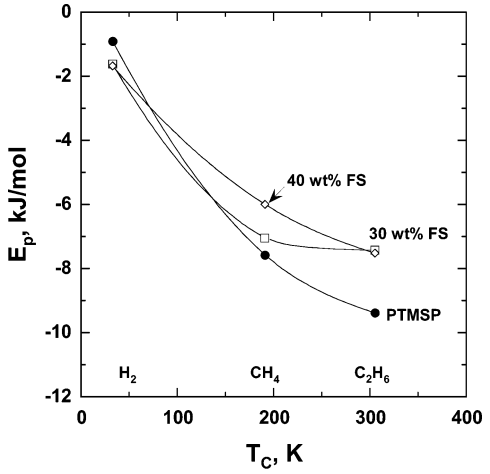

Figure 9. Activation energies of permeation in PTMSP containing 0, 30, and 40 wt % FS as a function of penetrant critical temperature. Permeation data were obtained with a feed pressure of 4.4 atm and a permeate pressure of 1 atm.

contrast, for PTMSP there is no systematic variation of penetrant activation energy of permeation with FS content. This difference in behavior relative to PMP is not entirely unexpected given the polymers' respective selectivity data and is probably related to the increased influence of non-solution-diffusion transport (i.e., pore-like transport) in filled PTMSP. As PTMSP is filled and the solution process becomes less important to transport, the large exothermic impact of ΔH_S on E_P is reduced (except for H_2 where ΔH_S is already quite small). At the same time, Knudsen flow, a nonactivated process, has a temperature dependence that is weak ($\propto \sqrt{1/T}$) and independent of penetrant structure.[28] Thus, it is reasonable for CH_4 and C_2H_6 E_P values to become less exothermic in going from PTMSP to PTMSP containing 40 wt % FS, and in fact this does appear to be the case (for instance, ethane's E_P increases from −9.4 kJ/mol in PTMSP to −7.5 kJ/mol in the 40 wt % FS sample), although the changes are near the uncertainty of the measurements.

To summarize the permeation results, the differences in the effect of FS addition on the selectivity and energetics of transport in PMP and PTMSP are probably related to the relative free volume present in the base polymers and the transport mechanisms that are dominant in the filled polymers. For PMP, FS addition increases polymer free volume and decreases diffusivity selectivity, yet even at the highest FS loading solution-diffusion transport (which permits vapor selectivity) predominates. In PTMSP, a similar increase in free volume occurs. However, since PTMSP has more free volume to begin with, FS addition permits access to the pore flow regime where the effects of Knudsen transport (which are detrimental to vapor selectivity) become progressively more important.

Solubility. Figure 10 presents sorption isotherms for H_2, N_2, CH_4, C_2H_6, C_3H_8, and n-C_4H_{10} in PTMSP and PTMSP containing varying amounts of FS. Consistent with previous reports for PTMSP,[26,40] penetrant sorption levels are very high in this polymer. For example, at 10 atm, the amount of N_2 sorbed by PTMSP (10 cm^3 (STP)/cm^3) is approximately 10 times that sorbed by polycarbonate, a conventional glassy polymer, or poly(dimethylsiloxane), a highly permeable rubbery polymer. PTMSP's enormous sorption capacity has been attributed to its very high free volume and resulting "spongelike" microporosity.[26] Among the different penetrants examined, solubility in PTMSP increases with increasing penetrant critical temperature, T_C, which is a typical result in the absence of specific polymer−penetrant interactions. The curvature exhibited by the isotherms in Figure 10 is consistent with a wealth of data on sorption in PTMSP[26,40,41] and has been described by models for sorption in dense glassy polymers as well as microporous adsorption models.[21]

Sorption isotherms in blends of PMP and FS were essentially the same as isotherms in pure PMP.[9] On the basis of the data in Figure 10, this result is also observed for penetrant sorption in PTMSP containing FS. For all penetrants, sorption levels in PTMSP and PTMSP containing up to 50 wt % FS are equivalent within typical sample variability and measurement uncertainty. This result indicates that all of the increase in permeability upon filling PTMSP is related to increased penetrant diffusion coefficients. Figure 10f highlights *n*-butane sorption in PTMSP, PTMSP containing 50 wt % FS, and adsorption on TS-530 FS powder. *n*-Butane uptake in PTMSP is very high compared to that sorbed on FS or by other polymers. For example, at 0.7 atm, the amount of *n*-butane sorbed by PTMSP, PMP, and TS-530 FS is 63, 45, and 13 cm^3 (STP)/cm^3, respectively. According to the additive solubility model in eq 10, and the fact that *n*-butane is the most soluble penetrant examined, the data in Figure 10f should exhibit the largest absolute difference in sorption levels between pure PTMSP and a nanocomposite. However, the *n*-butane isotherms in PTMSP containing 0 and 50 wt % FS are nearly coincident. The dashed line in Figure 10f represents the predicted *n*-butane uptake by PTMSP containing 50 wt % FS based on the sorption capacities of pure polymer and filler and the additive solubility model (eq 10). Similar to results in filled PMP,[9] the actual *n*-butane uptake in PTMSP containing 50 wt % FS is higher than predicted by the additive model, suggesting that the nanocomposite contains more sorption capacity than the sum of that supplied by its two constituents. This increased sorption capacity represents additional accessible free volume created by FS addition where penetrant molecules may be accommodated.

Diffusivity. From the equilibrium permeation and sorption data, penetrant concentration-averaged effective diffusion coefficients were calculated according to eq 2. Figure 11 presents these diffusion coefficients for H_2, CH_4, C_3H_8, and n-C_4H_{10} in PTMSP and FS-filled PTMSP as a function of penetrant concentration in the films. Consistent with previous reports for PTMSP,[40,41] diffusion coefficients are very high in this polymer. For example, the methane diffusion coefficient in PTMSP is approximately an order of magnitude higher than the corresponding value in PMP[9] and 4 orders of magnitude higher than that in poly(vinyl chloride),[47] a conventional low-free-volume glassy polymer. Even for PMP containing 30 wt % FS, the methane diffusion coefficient (1.2×10^{-5} cm^2/s)[9] is still lower than that in unfilled PTMSP (4.1×10^{-5} cm^2/s). This result emphasizes the extremely high diffusivities in PTMSP (higher even than those in filled PMP, which have been augmented by FS addition).

Within the uncertainty in the measurements, hydrogen diffusion coefficients are independent of penetrant concentration in PTMSP, while those of methane increase slightly with increasing penetrant concentration.

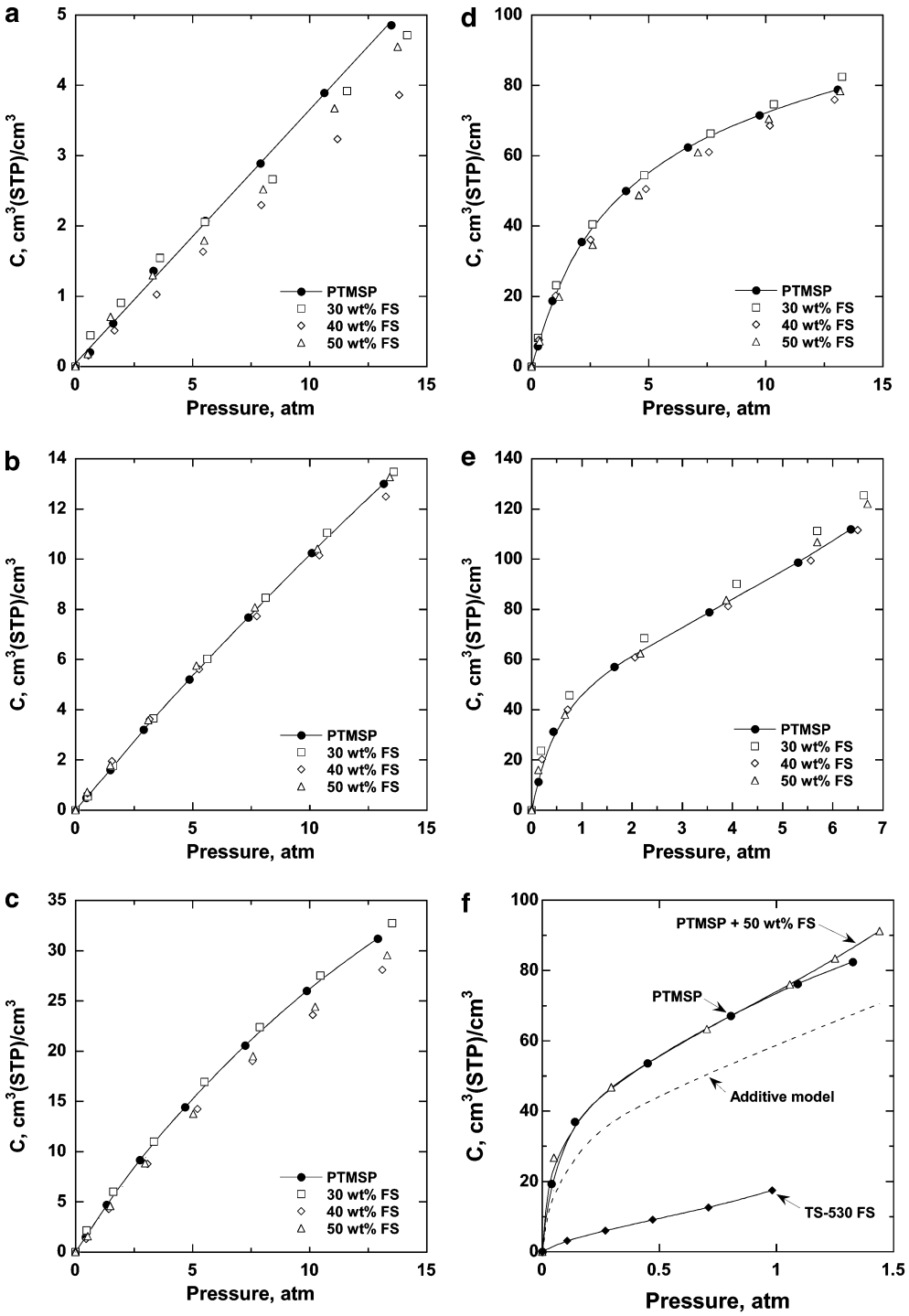

Figure 10. Sorption isotherms at 25 °C for (a) hydrogen, (b) nitrogen, (c) methane, (d) ethane, and (e) propane in PTMSP containing 0, 30, 40, and 50 wt % FS. (f) *n*-Butane sorption isotherms in PTMSP, PTMSP containing 50 wt % FS, and on TS-530 FS powder. The dashed line in (f) represents *n*-butane uptake in PTMSP containing 50 wt % FS as predicted by eq 10. The solid lines in (a−e) are smooth fits to the unfilled polymer data and serve as guides for the eye. The concentration of penetrant sorbed reported on the *y*-axis is per cm^3 of material (polymer + FS filler).

Such behavior is common for nonplasticizing penetrants in a glassy polymer.[18] For more soluble propane and *n*-butane, diffusion coefficients in unfilled PTMSP increase somewhat more strongly with increasing penetrant concentration, which is typical behavior for plasticizing penetrants. Interestingly, the concentration dependence of propane and *n*-butane diffusion coefficients is strongest for PTMSP and decreases with increasing FS content. This result is consistent with the permeation data, suggesting less penetrant-induced plasticization of filled PTMSP relative to unfilled PTMSP.

On the basis of the data in Figure 11, penetrant diffusion coefficients in PTMSP increase systematically with increasing FS content, essentially mirroring the permeability data (cf. Figure 3). This result is in agreement with findings for filled PMP, where FS addition increases free volume, thereby facilitating penetrant diffusion. Many of the diffusion coefficients in PTMSP and filled PTMSP are higher than those

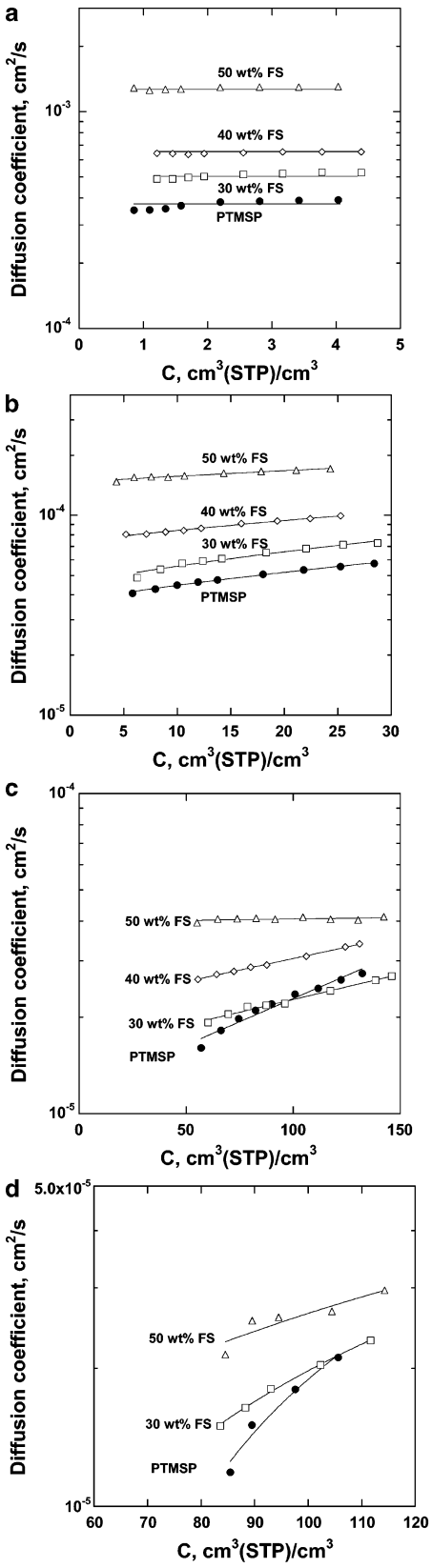

Figure 11. Diffusion coefficients of (a) hydrogen, (b) methane, (c) propane, and (d) *n*-butane in PTMSP containing 0, 30, 40, and 50 wt % FS at 25 °C as a function of penetrant concentration in the film.

typically observed for solid-phase diffusion ($<10^{-5}$ cm^2/s) and of the same order of magnitude as those found for surface diffusion (10^{-3}–10^{-6} cm^2/s).[48] Some diffusion coefficients in filled PTMSP approach and even exceed 10^{-3} cm^2/s (e.g., H_2 in the 50 wt % FS sample), a boundary characteristic of free phase transport mechanisms such as Knudsen flow.[49] This result is consistent with the reduced vapor/permanent-gas selectivity in filled PTMSP and the notion that this behavior is related to FS increasing the free volume in PTMSP beyond the solution-diffusion realm commonly observed in conventional, nonporous, dense polymer films.

Conclusions

The addition of nanoscale FS to high-free-volume, glassy PTMSP increases permeability and diffusivity, effects contrary to those reported in traditional filled polymer systems but similar to those observed in filled PMP, a structurally similar substituted polyacetylene. FS addition has little effect on gas and vapor solubility in PTMSP-based nanocomposites. The permeability enhancement at a given FS loading decreases with increasing base polymer permeability for filled polyacetylenes, suggesting that as polymer permeability and free volume increase so does the ability of the polymer matrix to accommodate filler particles without chain packing disruption. In contrast to filled PMP, when PTMSP is filled, the permeability coefficients of small gases increase more than those of large penetrants. Consequently, PTMSP becomes less vapor selective with increasing FS loading, in contrast to PMP. The methane blocking ratio in mixed-gas experiments for PTMSP is reduced at high FS loadings. Activation energies of permeation for more condensable penetrants increase slightly with FS content in PTMSP, suggesting a declining influence of penetrant solution on the transport process. Penetrant diffusion coefficients are approximately an order of magnitude higher in PTMSP than in PMP. For light gases at high FS loadings, the diffusion coefficients in PTMSP-based nanocomposites approach values typically encountered for Knudsen diffusion.

Acknowledgment. The authors gratefully acknowledge partial support of this work by the National Science Foundation (DMI-9901788 and CTS-9803225) and the Department of Energy (DE-FG02-99ER14991).

References and Notes

(1) Jia, M.; Peinemann, K. V.; Behling, R. D. *J. Membr. Sci.* **1991**, *57*, 289–296.
(2) Kulprathipanja, S.; Neuzil, R. W.; Li, N. Separation of fluids by means of mixed matrix membranes. US Patent No. 4,740,219, 1988.
(3) Duval, J. M. *J. Membr. Sci.* **1993**, *80*, 189–198.
(4) Suer, M. G.; Bac, N.; Yilmaz, L. *J. Membr. Sci.* **1994**, *91*, 77–86.
(5) Mahajan, R.; Zimmerman, C. M.; Koros, W. J. In *Polymer Membranes for Gas and Vapor Separation: Chemistry and Materials Science*; Freeman, B. D., Pinnau, I., Eds.; American Chemical Society: Washington, DC, 1999; pp 277–286.
(6) Pinnau, I.; He, Z. Filled Superglassy Membrane. U.S. Patent No. 6,316,684, 2001.
(7) Merkel, T. C.; Freeman, B. D.; Spontak, R. J.; He, Z.; Pinnau, I.; Meakin, P.; Hill, A. J. *Science* **2002**, *296*, 519–522.
(8) Merkel, T. C.; Freeman, B. D.; He, Z.; Morisato, A.; Pinnau, I. *Proc. Am. Chem. Soc. Div. Polym. Mater.: Sci. Eng.* **2001**, *85*, 301–302.
(9) Merkel, T. C.; Freeman, B. D.; He, Z.; Pinnau, I.; Meakin, P.; Hill, A. J. *Chem. Mater.* **2003**, *15*, 109–123.
(10) van Amerongen, G. J. *Rubber Chem. Technol.* **1964**, *37*, 1065–1152.
(11) Barrer, R. M. In *Diffusion in Polymers*; Crank, J., Park, G. S., Eds.; Academic Press: London, 1968; pp 165–217.
(12) Nagai, K.; Masuda, T.; Nakagawa, T.; Freeman, B. D.; Pinnau, I. *Prog. Polym. Sci.* **2001**, *26*, 721–798.
(13) Wijmans, J. G.; Helm, V. D. *AIChE Symp. Ser.* **1989**, *85*, 74–79.
(14) Morisato, A.; Pinnau, I. *J. Membr. Sci.* **1996**, *121*, 243–250.

(15) Pinnau, I.; Toy, L. G. *J. Membr. Sci.* **1996**, *116*, 199−209.
(16) Freeman, B. D.; Pinnau, I. *Trends Polym. Sci.* **1997**, *5*, 167−173.
(17) Pinnau, I.; Casillas, C. G.; Morisato, A.; Freeman, B. D. *J. Polym. Sci., Part B: Polym. Phys.* **1996**, *34*, 2613−2621.
(18) Ghosal, K.; Freeman, B. D. *Polym. Adv. Technol.* **1994**, *5*, 673−697.
(19) Wijmans, J. G.; Baker, R. W. *J. Membr. Sci.* **1995**, *107*, 1−21.
(20) Fried, J. R.; Goyal, D. K. *J. Polym. Sci., Part B: Polym. Phys.* **1998**, *36*, 519−536.
(21) Rutherford, S. W. *Ind. Eng. Chem. Res.* **2001**, *40*, 1370−1376.
(22) Ash, R.; Barrer, R. M.; Pope, C. G. *Proc. R. Soc. London A* **1963**, *271*, 19.
(23) Rao, M. B.; Sircar, S. *J. Membr. Sci.* **1996**, *110*, 109−118.
(24) Way, J. D.; Roberts, D. L. *Sep. Sci. Technol.* **1992**, *27*, 29−41.
(25) Bradley, D. F.; Baker, R. W. *Polym. Eng. Sci.* **1971**, *11*, 284−288.
(26) Srinivasan, R.; Auvil, S. R.; Burban, P. M. *J. Membr. Sci.* **1994**, *86*, 67−86.
(27) Knudsen, M. *Ann. Phys. (Leipzig)* **1909**, *28*, 73.
(28) Reid, R. C.; Prausnitz, J. M.; Poling, B. E. *The Properties of Gases and Liquids*, 4th ed.; McGraw-Hill: New York, 1987.
(29) Maxwell, C. *Treatise on Electricity and Magnetism*; Oxford University Press: London, 1873; Vol. 1.
(30) Barrer, R. M.; Barrie, J. A.; Rogers, M. G. *J. Polym. Sci., Part A* **1963**, *1*, 2565−2586.
(31) Barrer, R. M.; Barrie, J. A.; Raman, N. K. *Polymer* **1962**, *3*, 605−614.
(32) Freeman, B. D.; Hill, A. J. In *Structure and Properties of Glassy Polymers*; Tant, M. R., Hill, A. J., Eds.; American Chemical Society: Washington, DC, 1998; pp 306−325.
(33) Kobayashi, Y.; Haraya, K.; Hattori, S.; Sasuga, T. *Polymer* **1994**, *35*, 925−928.
(34) Yampol'skii, Y. P.; Shantorovich, V. P.; Chernyakovskii, F. P.; Kornilov, A. I.; Plate, N. A. *J. Appl. Polym. Sci.* **1993**, *47*, 85−92.
(35) Consolati, G.; Genco, I.; Pegoraro, M.; Zanderighi, L. *J. Polym. Sci., Polym. Phys. Ed.* **1996**, *34*, 357−367.
(36) CAB-O-SIL TS-530 Treated Fumed Silica: Technical Data, Cabot Corp., 1991.
(37) Nagai, K.; Nakagawa, T. *J. Membr. Sci.* **1995**, *105*, 261−272.
(38) Stern, S. A.; Gareis, P. J.; Sinclair, T. F.; Mohr, P. H. *J. Appl. Polym. Sci.* **1963**, *7*, 2035−2051.
(39) Sanders, E. S.; Koros, W. J.; Hopfenberg, H. B.; Stannett, V. T. *J. Membr. Sci.* **1984**, *18*, 53−74.
(40) Merkel, T. C.; Bondar, V.; Nagai, K.; Freeman, B. D. *J. Polym. Sci., Part B: Polym. Phys.* **2000**, *38*, 273−296.
(41) Ichiraku, Y.; Stern, S. A.; Nakagawa, T. *J. Membr. Sci.* **1987**, *34*, 5−18.
(42) Stannett, V. T. In *Diffusion in Polymers*; Crank, J., Park, G. S., Eds.; Academic Press: New York, 1968; p 41−73.
(43) Koros, W. J.; Hellums, M. W. In *Encyclopedia of Polymer Science and Technology*; Kroschwitz, J. I., Ed.; 1990; p 1211.
(44) Zhou, S.; Stern, S. A. *J. Membr. Sci.* **1989**, *27*, 205−222.
(45) Nagai, K.; Toy, L. G.; Freeman, B. D.; Teraguchi, M.; Masuda, T.; Pinnau, I. *J. Polym. Sci., Part B: Polym. Phys.* **2000**, *38*, 1474−1484.
(46) Morisato, A.; He, Z.; Pinnau, I. In *Polymer Membranes for Gas and Vapor Separation: Chemistry and Materials Science*; Freeman, B. D., Pinnau, I., Eds.; American Chemical Society: Washington, DC, 1999; pp 56−67.
(47) Berens, A. R.; Hopfenberg, H. B. *J. Membr. Sci.* **1982**, *10*, 283−303.
(48) Smith, J. M. *Chemical Engineering Kinetics*; McGraw-Hill: Singapore, 1981.
(49) Ruthven, D. M. *Principles of Adsorption and Adsorption Processes*; John Wiley & Sons: New York, 1984.
(50) Shantarovich, V. P.; Kevdina, I. B.; Yampolskii, Y. P.; Alentiev, A. Y. *Macromolecules* **2000**, *33*, 7453−7466.

MA0341566